CANCER GENOMICS & PROTEOMICS *21*: 485-501 (2024)
doi:10.21873/cgp.20466

DNA Methylation in Recurrent Glioblastomas: Increased TEM8 Expression Activates the Src/PI3K/AKT/GSK-3β/B-Catenin Pathway

PARAMITA KUNDU[1,2], RUCHI JAIN[1,3], NANDAKI NAG KANURI[4], ARIVAZHAGAN ARIMAPPAMAGAN[5], VANI SANTOSH[4] and PATURU KONDAIAH[1]

[1]*Department of Molecular Reproduction, Development and Genetics, Indian Institute of Science, Bangalore, India;*
[2]*Breast Cancer Now Toby Robins Research Centre, Department of Breast Research, The Institute of Cancer Research, London, U.K.;*
[3]*Al Jalila Genomics Centre, Al Jalila Children's Hospital, Dubai, United Arab Emirates;*
[4]*Department of Neuropathology, National Institute of Mental Health and Neurosciences, Bangalore, India;*
[5]*Department of Neurosurgery, National Institute of Mental Health and Neurosciences, Bangalore, India*

Abstract. *Background/Aim: Glioblastomas (GBM) are infiltrative malignant brain tumors which mostly recur within a year's time following surgical resection and chemo-radiation therapy. Studies on glioblastoma cells following radio-chemotherapy, have been demonstrated to induce trans-differentiation, cellular plasticity, activation of DNA damage response and stemness. As glioblastomas are heterogenous tumors that develop treatment resistance and plasticity, we investigated if there exist genome-wide DNA methylation changes in recurrent tumors. Materials and Methods: Utilizing genome-wide DNA methylation arrays, we compared the DNA methylation profile of 11 primary (first occurrence) tumors with 13 recurrent (relapsed) GBM, to delineate the contribution of epigenetic changes associated with therapy exposure, therapy resistance, and relapse of disease. Results: Our data revealed 1,224 hypermethylated- and 526 hypomethylated-probes in recurrent glioblastomas compared to primary disease. We found differential methylation of solute carrier and ion channel genes, interleukin receptor/ligand genes, tumor-suppressor genes and genes associated with metastasis. We functionally characterized one such hypomethylated-up-regulated gene, namely anthrax toxin receptor 1/tumor endothelial marker 8 (ANTXR1/TEM8), whose expression was validated to be significantly up-regulated in recurrent glioblastomas compared to primary tumors and confirmed by immunohistochemistry. Using overexpression and knockdown approaches, we showed that TEM8 induces proliferation, invasion, migration, and chemo-radioresistance in glioblastoma cells. Additionally, we demonstrated a novel mechanism of β-catenin stabilization and activation of the β-catenin transcriptional program due to TEM8 overexpression via a Src/PI3K/AKT/GSK3β/β-catenin pathway. Conclusion: We report genome-wide DNA methylation changes in recurrent GBM and suggest involvement of the TEM8 gene in GBM recurrence and progression.*

Correspondence to: Paturu Kondaiah, Former Professor and Chair, Department of Molecular Reproduction, Development and Genetics, Indian Institute of Science, and Honorary Advisor, Sri Shankara Cancer Hospital and Research Centre, Bangalore, 560012, India. E-mail: paturu@iisc.ac.in

Key Words: β-catenin, DNA methylation, glioblastoma, tumor endothelial marker 8, recurrence, resistance.

A major bottleneck in glioblastoma (GBM, Grade IV glioma) treatment is the problem of recurrence. Recurrence in glioblastoma is inevitable (1) and invariably fatal. Owing to their highly infiltrative nature, it is virtually impossible to attain complete surgical debulking in GBM, in spite of gross total resection (GTR) of all contrast-enhancing areas on pre-operative MRIs. Tumor cells microscopically infiltrate beyond the contrast enhancing areas and to the contralateral hemisphere *via* the corpus callosum. Additionally, GBMs contain a peri-tumoral zone defined by tumor cell infiltration into the normal brain parenchyma. The extent of this zone is variable and therefore GTR is incapable of eliminating all residual tumor cells. Indeed, two-thirds of all recurrences occur locally, within a 3 cm margin (2) at a median time of 59.5 weeks (3).

Standard protocol for glioblastoma management entails a combination of maximal safe resection, chemotherapy

with temozolomide, and fractionated ionizing radiation (IR) to the tumor bed (4). While this regimen improves survival compared to surgery alone, it is increasingly shown that both IR and temozolomide may result in generation of therapy resistance. For instance, therapeutic concentrations of temozolomide exposure led to increase in stem-cells and more diffuse tumors (5, 6), trans-differentiation of bulk tumor cells to endothelial cells showing vasculogenic mimicry (7), and induced HIF1α signaling (6) in glioma cells. Exposure to therapeutically relevant (2-3 Grays) doses of IR showed an increase in stem-cell content and accelerated DNA-damage response (8), a marked decrease in differentiation markers (9), subtype plasticity from pro-neural to mesenchymal phenotypes (10), and induced HIF1α signaling (6). Much older studies (3) also show that radiographic implants at tumor beds accelerated the detection of new lesions in glioblastomas.

To explain the phenomena of inevitable recurrence in GBMs, it was proposed that infiltrated and residual tumor cells in the tumor-bed, termed recurrence initiating stem-cells (RISCs), serve as seeds for the recurrent disease (11). Given that GBM cells are inherently plastic, these cells are postulated to undergo adaptive responses to genotoxic therapy, resulting in therapy resistance commonly seen in recurrent GBMs. Local and distant recurrences also harbor distinct mutational patterns (12), suggesting a field cancerization effect whereby non-genetic mechanisms may also play a role in precipitating recurrences.

IR and temozolomide, apart from inducing genetic aberrations such as mutations (13), may also result in epigenetic changes, such as DNA methylation or histone modifications (14, 15). Additionally, the hypoxic nature of GBMs poses a dual challenge, it initiates proangiogenic signaling and dampens the IR response due to lack of O_2 radicals to 'fix' double-strand breaks. Interestingly, hypoxia also influences DNA methylation kinetics (16, 17). It is plausible that in this hypoxic, genotoxic GBM microenvironment, residual tumor cells undergo DNA methylation changes which may translate into clinically more aggressive and therapy-refractory tumors. In this study, utilizing Illumina's 450K Methylation Bead Array, we have compared the DNA methylome of glioblastoma (first occurrences/primary tumors) with recurrent tumors to understand if there exists DNA methylation changes that may impact the aggressiveness of recurrent tumors.

Utilizing the data generated from our cohort, we report that several genes are hyper- or hypomethylated in recurrent tumors, resulting in transcriptional changes. We have functionally characterized one such hypomethylated-up-regulated gene in recurrent tumors, *ANTXR1*/*TEM8*, and delineated the signaling mechanism responsible for its pro-tumorigenic actions in glioblastomas.

Materials and Methods

Patient characteristics. Tumor tissues were obtained from patients availing surgical treatment at the National Institute of Mental Health and Neurosciences (NIMHANS), Bangalore, after obtaining written informed consent and approval by the Institutional Ethics Committee of NIMHANS, dated NIMHANS/3rd IEC (BS & NS Div.)/2016. The study was performed according to the Declaration of Helsinki guidelines. A total of 24 fresh-frozen tissues were utilized in the study, consisting of 11 treatment-naïve (primary) GBMs and 13 relapsed (recurrent) GBMs, of which 10 samples belonged to patient-matched pairs (5 pairs) (Table I). The inclusion criteria were treatment-naïve and relapsed Isocitrate Dehydrogenase-wildtype (IDH-wt) glioblastomas, while the exclusion criteria were glioblastomas of IDH-mutant origin. Tumors were verified to be grade IV glioblastoma by a neuropathologist, and wildtype-IDH status was confirmed by PCR for R132H.

Cell lines. Cell lines of Grade IV astrocytoma origin, such as U87-MG, A172, U251, LN229 originally obtained from European Collection of Authenticated Cell Cultures (ECACC), were recently verified by short tandem repeat analysis (DNA Labs, Hyderabad, India). Cells were grown in high-glucose DMEM with 10% newborn calf serum with 1X Penicillin-Streptomycin, in a humidified incubator at 37°C and 5% CO_2. For overexpression studies, an expression construct containing TEM8 cDNA (3X-Flag-hTEM8 pcDNA3.1) was transfected using Lipofectamine 3000 (Thermo Fisher Scientific, Waltham, MA, USA) and cells were selected with G418-disulfate (#G8168, Sigma-Aldrich, MA, USA) for a month. For knockdown expression, cells were virally transduced and selected with Puromycin dihydrochloride (#540222, Sigma). Lentiviral packaging was performed in HEK293T (ATCC) cells using target plasmids encoding shRNA sequences and helper plasmids psPAX2 and pMD2.G.

Genomic DNA and protein isolation from patient samples. Fresh-frozen patient tissues were utilized to isolate genomic DNA using Genomic DNA Extraction kit (Qiagen, Venlo, the Netherlands) according to manufacturer's instructions and run on 1% Agarose gel to verify integrity of DNA. For protein isolation from glioblastoma samples, 30 mg of tissue was weighed, minced, and mixed with fresh lysis buffer containing protease inhibitors, and processed in a TissueLyser II (#85300, Qiagen) machine for 3-5 cycles (30 Hz, 30 s on, 30 s off) till a non-viscous lysate was obtained. The lysate was spun for 30' to isolate protein, run on an SDS-PAGE gel and stained with Coomassie Brilliant Blue to verify protein integrity.

450K DNA Methylation Array. Genomic DNA isolated from patients were subjected to Infinium 450K Bead Array (Illumina Inc., San Diego, CA, USA) that interrogates ~485,577 CpG sites across the human genome, according to manufacturer's instructions. The β-value for a particular CpG probe was used as a measure of differential methylation across primary and recurrent samples, with probes showing $|\Delta\beta|=0.2$ with $p\leq0.05$ being designated as differentially methylated regions (DMRs). $\Delta\beta \leq -0.2$ were considered as hypomethylated probes and $\Delta\beta \geq +0.2$ were considered as hypermethylated probes respectively, in recurrent tumors.

Methylation array data analysis. The Combat pipeline in ChaMP package (18) was implemented for pre-processing and batch correction of samples in BioConductor. Wilcoxon rank-sum test with *p*-value

Table I. *Clinical characteristics of patient samples for methylation array.*

Sr. No.	Age/Sex	Annotation	Diagnosis	Histopathology	Pair status	R132H status
1	62/M	GBM 1	Primary	Glioblastoma	Paired with GBM 5	Negative
2	30/M	GBM 2	Primary	Glioblastoma	Paired with GBM 6	Negative
3	40/M	GBM 3	Primary	Glioblastoma	Paired with GBM 7	Negative
4	48/M	GBM 4	Primary	Glioblastoma	Paired with GBM 8	Negative
5	62/M	GBM 5	Relapsed	Recurrent glioblastoma	Paired with GBM 1	Negative
6	30/M	GBM 6	Relapsed	Recurrent glioblastoma	Paired with GBM 2	Negative
7	40/M	GBM 7	Relapsed	Recurrent glioblastoma	Paired with GBM 3	Negative
8	48/M	GBM 8	Relapsed	Recurrent glioblastoma	Paired with GBM 4	Negative
9		GBM 9	Primary	Glioblastoma	Paired with GBM 10	Negative
10		GBM 10	Relapsed	Recurrent glioblastoma	Paired with GBM 9	Negative
11	64/M	GBM 11	Relapsed	Recurrent glioblastoma	Unpaired	Negative
12	40/M	GBM 12	Relapsed	Recurrent glioblastoma	Unpaired	Negative
13	60/M	GBM 13	Relapsed	Recurrent glioblastoma	Unpaired	Negative
14	43/M	GBM 14	Relapsed	Recurrent glioblastoma	Unpaired	Negative
15		GBM 15	Relapsed	Recurrent glioblastoma	Unpaired	Negative
16		GBM 16	Relapsed	Recurrent glioblastoma	Unpaired	Negative
17		GBM 17	Relapsed	Recurrent glioblastoma	Unpaired	Negative
18		GBM 18	Relapsed	Recurrent glioblastoma	Unpaired	Negative
19	60/M	GBM 19	Primary	Glioblastoma	Unpaired	Negative
20	61/M	GBM 20	Primary	Glioblastoma	Unpaired	Negative
21	47/F	GBM 21	Primary	Glioblastoma	Unpaired	Negative
22	63/F	GBM 22	Primary	Glioblastoma	Unpaired	Negative
23	63/M	GBM 23	Primary	Glioblastoma	Unpaired	Negative
24	72/M	GBM 24	Primary	Glioblastoma	Unpaired	Negative

R132H denotes IDH mutation status. M: Male, F: female.

cutoff of 0.05 was employed for finding differential methylation at CpG probes. Gene-level annotations at 5'-UTR (Untranslated region), 1st Exon, TSS 200 (Transcription Start Site) and TSS 1500 were conducted using Illumina Methylation analyzer package (IMA). The Seaborn package was used to generate hierarchical clustering for the top ~50 hypomethylated- and hypermethylated probes. The 450K methylation array data is deposited in Gene Expression Omnibus (GEO) with accession number GSE190953.

Inhibitor experiments. Cells were serum-starved for 24 h before inhibitor treatment for 6 h and subsequent protein collection. Small-molecule inhibitors used were synthetic RGD peptide (10 μM, GRDGNP, #14501, Cayman Chemicals, Ann Arbor, MI, USA), ILK inhibitor (1 μM, CPD-22, Calbiochem, Merck, Boston, MA, USA), PI3 Kinase inhibitor LY294002 (10 μM, #440202, Calbiochem), FAK inhibitor-1 (10 μM, #324877, Calbiochem), Src inhibitor PP2 (10 μM #529573, Calbiochem) and Src inhibitor inactive analog PP3 (10 μM, #529574, Calbiochem).

Semi-quantitative and quantitative real time PCR. Total RNA from cell lines and patient samples was isolated using TRI reagent (Sigma-Aldrich). 2 μg of total RNA was converted to cDNA using High-Capacity cDNA Archive kit (Applied Biosystems, Bedford, MA, USA). Semi-quantitative and real-time PCRs were performed using DreamTaq Mastermix (Thermo Scientific) and DyNamo ColorFlash SYBR Green Mastermix (Thermo Scientific) respectively. Fold changes were calculated using the ΔΔCT method. Primer sequences are given in Table II. RPL-35A was used for normalization as it was reported to be un-regulated in glioblastomas (19).

Immunohistochemistry. A retrospective cohort of 29 pairs of formalin-fixed paraffin embedded IDH-wildtype primary and recurrent glioblastomas was utilized to assess TEM8 protein expression (Tris-EDTA buffer, 1:500 ab21270 TEM8 antibody, Abcam, Cambridge, UK). Tissue microarrays for control brain tissue (from temporal cortex surgically removed in patients with drug resistant epilepsy: 'control') was utilized to assess TEM8 expression. Briefly, 4 μM slices were deparaffinized using Xylene and 100% Methanol, followed by heat-mediated antigen-retrieval at 900W-5', 600W-10', 450W-5'. Endogenous peroxidase was quenched with 5% H_2O_2 in Methanol for 20 min and subsequently blocked with 5% skimmed milk for 1 h. After overnight incubation at 4°C, slides were developed using PolyExcel HRP/DAB Detection System Universal kit (PathnSitu Biotechnologies, CA, USA), counterstained with hematoxylin, dried and mounted using DPX (Sigma-Aldrich). A semi-quantitative labeling index method was employed to assess overall staining: 2+ and 1+ denoted strong and moderate staining respectively, while the percent of cells stained was noted separately. A combined score was allotted [(2+ staining intensity * percent positive cells) + (1+ staining intensity * percent positive cells)] to each sample. Pair-wise comparison using Wilcoxon signed-rank test was employed for test of significance.

Plasmids. 3X-Flag-hTEM8 (pcDNA3.1) was a kind gift from Brad St. Croix, National Institutes of Health, USA (20). M50 Super 8X TOPFlash and M51 Super 8X FOPFlash and pRLTK were obtained from Addgene (gift from Randall Moon). TEM8 shRNAs (D6 5'CCGGCCCACAGTTGAGAATGTCCTTCTCGAGAAGGACAT TCTCAACTGTGGGTTTTTG 3' and D9 5'CCGGACACTCAAT

Table II. *List of gene specific primers used in the study.*

	Forward primer (5'-3')	Reverse primer (5'-3')	Amplicon (bp)	Tm (°C)
OCT4/POU5F1	ACATCAAAGCTCTGCAGAAAGAACT	CTGAATACCTTCCCAAATAGAACCC	127	60
TWIST1	GTCCGCAGTCTTACGAGGAG	CCAGCTTGAGGGTCTGAATC	159	60
β-Catenin	CACAAGCAGAGTGCTGAAGGTGC	AAGGAGGCCTTCCATCCCTTC	190	60
AXIN2	CCGAGATCCAGTCGGTGATG	GGTTGGCGAAAGTTTGCACT	212	60
NANOG	CCTCCTCCATGGATCTGCTTATTCA	CAGGTCTTCACCTGTTTGTAG	262	60
ZEB1	TGCACTGAGTGTGGAAAAGC	TGGTGATGCTGAAAGAGACG	237	60
ANTXR1	AGGTTCGTTGGGGAGAAAAGG	CAGTAGGACCCACAAGGCAT	200	60
ASAP1	TGACTAGCAAAACGCAGAACC	ACACACATTATATCCCCCTCC	152	60
CNOT7	CTCAGCGACACAAGTACATAAATAA	TGGCATAGTGAGGGCACAAG	114	60
LRP6	CCGAGTCAGAACCTGGAAATAC	CTCCAACTGATCTCCCATCTAATC	127	60
GAPDH	TTAAAAGCAGCCCTGGTGAC	CTCTGCTCCTCCTGTTCGAC	144	60
RPL35A	GAACCAAAGGGAGCACACAG	CAATGGCCTTAGCAGGAAGA	236	50
WNT1	GGTTTCTGCTACGCTGCTG	TAAGCAGGTTCGTGGAGGAG	113	60
WNT2	GAAGCCAACGAAAAATGACC	CCCACAGCACATGACTTCAC	148	50
WNT4	GCGAGCAACTGGCTGTACC	GAGTCCCTTGCGTCACCAC	256	65
WNT11	ATATCCGGCCTGTGAAGGACTC	TCTTGTTGCACTGCCTGTCTTG	114	65
ACTA2/αSMA	CAGCCAAGCACTGTCAGG	CAATGGATGGGAAAACAGC	150	60

Tm indicates annealing temperature of primers.

GAGAAGCCCTTTCTCGAGAAAGGGCTTCTCATTGAGTGTTT TTTG 3') and scrambled shRNA plasmids were obtained from Sigma's Mission® shRNA Library in lentiviral pLKO.1 background (kindly provided by Prof. G. Subba Rao, IISc).

Wound-healing and invasion assays. Wound-healing assays were conducted on confluent monolayers by making a scratch with a p200 tip, in the presence of 0.5-1 μM Mitomycin C to control for proliferation differences. Images were analyzed using TScratch software (21). Invasion assays were performed according to manufacturer's instructions using BioCoat Matrigel 8 μM Invasion chambers (#354481, Corning, Corning, NY, USA) by seeding 75,000-200,000 cells in triplicates.

MTT assays. MTT assays (MTT (3-(4,5-Dimethylthiazol-2-yl)-2,5-Diphenyltetrazolium Bromide, #M2128; Sigma-Aldrich) were performed to assess relative chemoresistance of vector control/scrambled cells and overexpressing/knockdown cells against Temozolomide, Cisplatin, Etoposide, and 5-Fluorouracil. Briefly, 5,000 cells were plated and treated with drugs for 72 h. Post-treatment, 20 μl MTT reagent (5 mg/ml) was added and incubated for a further 3.5 h. Formazan crystals that were formed, was dissolved in DMSO (Sigma) and absorbance measured at 570 nm. The data was normalized to solvent (DMSO)-treated controls and a non-linear regression curve was fitted using GraphPad Prism 5.0 to arrive at 50% relative Inhibitory Concentration (IC_{50}) values.

BromodeoxyUridine incorporation assays. BrdU incorporation assay was performed according to manufacturer's guidelines (Calbiochem, Cat. No.: QIA58). Briefly, 1,000-2,000 cells were plated in triplicates in 96 well plates and allowed to attach overnight. 20 μl of a diluted BrdU stock (1:2,000) was added to the wells for 4 h, after which cells were washed with PBS, and fixed with fixation-denaturation solution for 30 min. After fixation, wells were incubated with anti-BrdU primary antibody for 2 h, washed twice with PBS and incubated with peroxidase IgG-HRP for 1 hour. After three washes, 100 μl of chromogenic substrate TMB was added and incubated in the dark for 15 min. The reaction was terminated by adding 2.5N H_2SO_4 and yellow absorbance was measured at 450-540 nm using a Plate Reader (Tecan, Mannedorf, Switzerland).

Cell cycle and proliferation assays. Equal number of cells were plated in triplicates and allowed to attach overnight. Cells were then serum-starved with serum-free DMEM media for 72 h to achieve cell cycle synchronization. Post 72 h, one set of cells were harvested, fixed with Ethanol, and stored in –20˚C (denoted as 0 h). The other set was stimulated with 10% fetal bovine serum containing media, *i.e.*, complete media for another 12 h and allowed to progress through the cell cycle, harvested (denoted as 12 h) and stored at –20˚C. A 10 μg/ml Propidium Iodide solution containing RNase A (Thermo Scientific) was used to stain the cells at 37˚C and 10,000 events were captured in BD FACSVerse (BD Biosciences). The data was analyzed using BD FACS Suite software. For proliferation assays, equal number of cells were plated in 6 well-plates in triplicates and allowed to attach overnight. Cell proliferation was measured after trypsinization, using a Trypan-blue exclusion assay with ViCell XR (Beckman Coulter) at 24, 48 and 72 h of growth.

Western Blotting. For immunoblotting, protein was harvested using a modified RIPA buffer containing 1X Protease-Inhibitor Cocktail (Set III, Calbiochem), and quantified using Bradford reagent (Biorad, Hercules, CA, USA). Equal amount of protein was electrophoresed on a 12.5% Sodium Dodecyl Sulfate-Polyacrylamide gel and transferred onto a 0.45 μM polyvinylidene difluoride membrane (Immobilon-P, Merck). The membrane was blocked with 3% bovine serum albumin for 1 hour. Primary antibodies used were: Anti-TEM8 (#73136, Santa Cruz Biotechnology, Santa Cruz, CA, USA), Phospho GSK3β S9 [#9323, Cell Signaling Technology (CST), Danvers, MA, USA], Total GSK3β (#9315, CST), Phospho FAK Y397 (#3284 , CST), Total

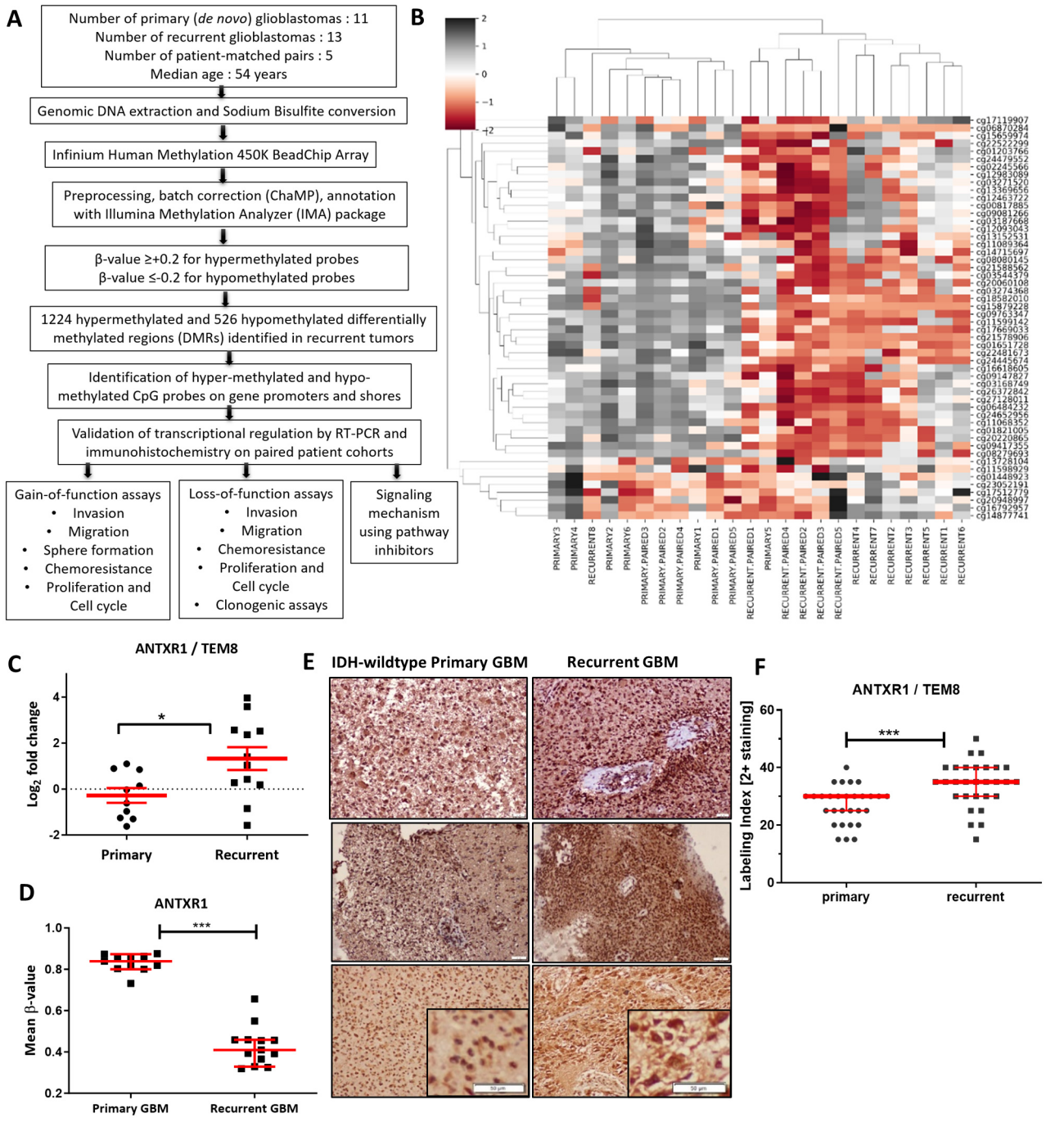

Figure 1. *Continued*

FAK (#3285, CST), Phospho-Akt S473 (#4060, CST), Phospho-Akt T308 (#9275, CST), Total Akt (#9272, CST), β-catenin (#C2206, Sigma), Lamin A/C (#4777, CST) and β-Actin (#A5441, Sigma), Vimentin (#V2258, Sigma), Oct4 (#ab19857, Abcam), Zeb1 (#3396, CST), Twist (#ab50887, Abcam), α-SMA (#5694, Abcam), phospho-ILK S246 (#AB1076, Millipore), Total ILK (#3862, CST). Membranes were developed using femtoLUCENT-PLUS HRP (#786-003, G Biosciences, Overland, MO, USA) in a Chemi-Doc (Biorad). For nuclear-cytoplasmic fractionation, a hypotonic lysis buffer protocol was used (22).

Dual luciferase assays. 500 ng of Super 8X TOPFlash (containing TCF binding elements) or FOPFlash (containing mutated binding sites) was co-transfected with 10 ng of pRL-TK (Renilla luciferase-thymidine kinase) in U87 or LN229 cells. After 48 h, lysates were harvested using passive lysis buffer and luminescence measured

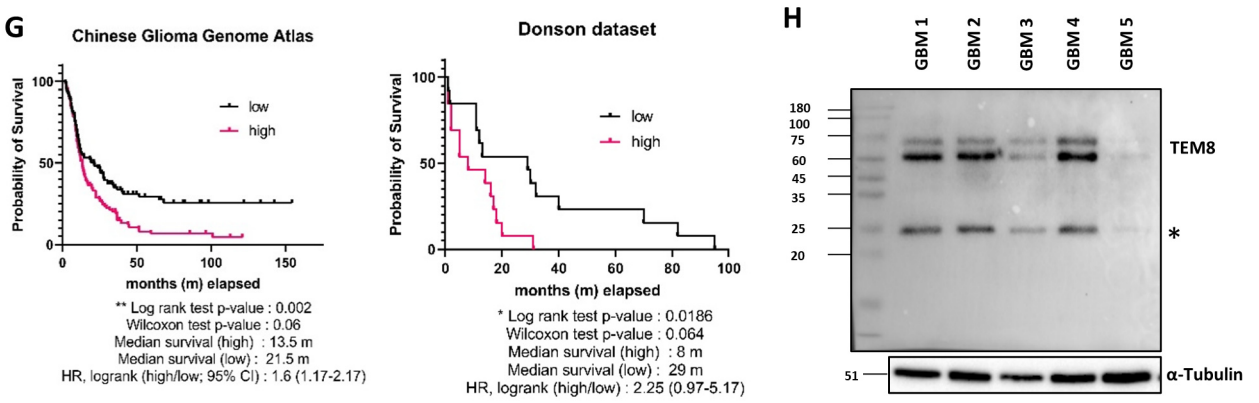

Figure 1. *The ANTXR1/TEM8 gene is up-regulated in recurrent glioblastomas. (A) A brief overview of analysis of differentially methylated regions in primary and recurrent glioblastomas. (B) Hierarchical clustering for the top ~50 hypomethylated probes in recurrent vs. primary tumors. (C) Relative expression of hypomethylated genes ANTXR1/TEM8, normalized by RPL-35A in our cohort of primary and recurrent glioblastomas. (D) Mean β-value of ANTXR1 promoter-localized probe in primary and recurrent samples. (E) Representative images of immunohistochemistry staining of TEM8 in a retrospective cohort of paired primary and recurrent GBM tissues. (F) Labeling index for TEM8 immunostaining in paired samples; Wilcoxon signed rank paired test p-value 0.001. (G) Kaplan-Meier survival curves for ANTXR1/TEM8 in the Chinese Glioma Genome Atlas (CGGA) and Donson datasets, classified according to high and low mRNA expression in glioma patients. Hazard ratio (HR) calculated as low/high, with log-rank (Mantel-Cox) and Wilcoxon (Gehan-Breslow-Wilcoxon) p-values reported. (H) TEM8 expression in five GBM patient tissues. Note the predominant ~63 kDa isoform, representing the transmembrane bound receptor. The extra band at 25 kDa (*) is presumably a cleavage product.*

according to Promega's Dual Luciferase Assay kit (#E1980, Promega) guidelines.

Zymography. Gelatin zymography was employed to assess levels of matrix metalloproteinases in 72 h serum-free conditioned media from overexpressing cells. Briefly, 40 μl of media was mixed with 5X non-reducing sample buffer and electrophoresed on Gelatin (0.1%)-SDS-8% Polyacrylamide gel. The gels were washed twice with washing buffer and incubated in developing buffer for 22 h at 37˚C and subsequently stained with Coomassie Brilliant Blue.

Neurosphere assays. Neurospheres were plated as single-cell suspensions in ultra-low attachment 24-well plates for 7-14 days using Neurobasal media (Invitrogen) supplemented with 3 mM L-Glutamine (Invitrogen), 1X B27 supplement (Life Technologies, Carlsbad, CA, USA), 0.5X N2 supplement (Life Technologies), 2 μg/ml Heparin (Sigma), 20 ng/ml recombinant human EGF (R&D systems), 20 ng/ml recombinant human FGF2 (Peprotech, Cranbury, NJ, USA), and 1X Penicillin-Streptomycin-Amphotericin B (Invitrogen). Images were analyzed in Fiji (23) to calculate number and mean diameter of spheres.

Clonogenic assays. A γ-irradiator with $Cobalt_{60}$ source (Blood Irradiator 2000, BRIT) was used to irradiate cells with 0, 2, 4, 6, 8, 10 Grays. A single-cell suspension was plated in triplicates in 6-well plates and allowed to grow for three weeks. Colonies were fixed, stained with Crystal Violet, and photographed at 600 dpi using Chemidoc (Biorad). Images were processed in Fiji using Threshold > Process > Binary > Watershed > Analyze particles. The plating efficiency (PE) and surviving fraction (SF) was calculated as:

PE=(Number of colonies at each dose)/ (Number of cells plated for that particular dose)

SF at a particular dose=(PE at a particular dose)/(Maximum PE)

The SF was plotted at log scale to fit the data to a linear-quadratic model. Experiments were conducted thrice, and representative data is shown.

Statistical analysis. Statistical analyses were conducted using GraphPad Prism 5. For qPCR fold change calculation, Mann-Whitney two-tailed *t*-tests were conducted using $p \leq 0.05$ for significance ($^{*}p \leq 0.05$, $^{**}p \leq 0.001$, $^{***}p \leq 0.0001$). For analysis of paired samples, Wilcoxon signed rank test and paired t-tests were conducted. Unpaired Student's *t*-test was conducted for all other analysis.

Data availability statement. The datasets generated in this study are deposited in Gene Expression Omnibus with accession number GSE190953.

Results

Genome-wide DNA methylation changes in primary and recurrent glioblastomas. A brief overview of investigating differentially methylated regions (DMRs) in primary and recurrent glioblastoma samples, and subsequent *in vitro* experimental analyses is depicted in Figure 1A. Genomic DNA were subjected to sodium bisulfite conversion and subsequently the Infinium 450K Methylation Bead Array was performed for assessing DMRs with a Δβ-value cutoff of |0.2| and $p \leq 0.05$, revealing 1224 hypermethylated and 526 hypomethylated probes (Supplementary Table I), where $|\Delta\beta| \geq +0.2$ in recurrent tumors compared to primary is considered to be hypermethylated while $|\Delta\beta| \leq -0.2$ in recurrent tumors compared to primary is considered to be hypomethylated at that particular CpG locus. We performed a gene-level annotation for these commonly regulated DMRs for probes localizing to promoter-proximal regions, such

as 5'-Untranslated Regions, Transcription Start Site (TSS) 200 and TSS 1500, and 1st Exon regions. The top ~50 hypo/hypermethylated promoter-proximal probes, listed in Supplementary Table II; were subjected to unsupervised hierarchical clustering. The resulting clustered hypomethylated probes is represented in Figure 1B.

The clustering results revealed that the recurrent (RECURRENT 1-8, and RECURRENT.PAIRED 1-5) and primary samples (PRIMARY 1-6 and PRIMARY.PAIRED 1-5) clustered separately in case of the hypomethylated probes, except for sample 'RECURRENT 8' that clustered with primary samples. However, for the hypermethylated probes (Supplementary Figure 1A), the clustering did not differentiate between primary and recurrent samples, suggesting that promoter hypomethylation is a more uniform DNA methylation change in recurrent tumors on disease progression.

We observed several interesting candidates among our list of differentially regulated genes, categorized according to reported functions in Supplementary Figure 1B. Several genes, such as *CAV2*, *HTATIP2*, *DSC3* for which epigenetic inactivation in different cancers is reported (24–26), came up as hypermethylated genes in recurrent tumors. Genes associated with histological grade, such as *ZHX2*, *ASAP1* and genes with reported protumorigenic functions, such as *ANTRX1/TEM8, FAM46D, AZIN1*, *CNOT7* were hypomethylated. Several genes encoding solute carrier ion channels or potassium channels (*KCNN3, KCNT1, KCNQ1*) were dysregulated (hypo/hypermethylated) in recurrent glioblastomas. This is interesting because involvement of ion channels in gliomagenesis is increasingly being noted (27), and this data may suggest that there could be unexplored contribution of ion channel dysregulation in glioblastoma progression.

We validated randomly selected hypomethylated genes in our patient cohort and found them to be transcriptionally up-regulated in recurrent glioblastomas. These include stem-cell biomarker *ANTXR1/TEM8* (Figure 1C) and the transcriptional co-repressor *CNOT7* (Supplementary Figure 1C). We decided to functionally characterize the *ANTXR1/TEM8* (Anthrax Toxin Receptor 1/Tumor Endothelial Marker 8) gene as it was found to be hypomethylated at a promoter-associated CpG island at TSS200, suggesting that hypomethylation could potentially regulate its transcription, apart from the fact that it is characterized as a stem-cell biomarker in triple negative breast cancer (28). It is also reported to be pro-tumorigenic in osteosarcomas, colorectal and gastric cancer (29–31), although, significance of its expression or its role in glioblastomas is not yet reported.

As the *ANTXR1/TEM8* gene was found to be hypomethylated in recurrent glioblastomas and transcriptionally up-regulated in recurrent glioblastomas, we assessed whether the TEM8 protein is overexpressed in paired recurrent glioblastomas compared to primary tumors. To this end, a separate retrospective cohort of 29 patient-matched (paired) primary and recurrent glioblastomas was utilized to determine protein expression *via* immunohistochemistry. We found significant up-regulation of protein expression (Wilcoxon paired signed-rank test, p=0.001) in recurrent tumors compared to primary tumors (Figure 1D), with a mean labelling index of 34.5 in recurrent samples compared to 27 in primary samples (Figure 1E, Supplementary Figure 1D). The differentially methylated promoter proximal CpG in the ANTXR1 TSS200 (cg06870284) was found to have lower mean β-value in recurrent tumors compared to primary ones (Figure 1F), suggesting that the increased protein and RNA expression could be due to promoter-proximal hypomethylation. In glioblastomas, the role or consequence of TEM8 expression is unknown. Survival analysis *via* Gliovis (32) revealed that higher TEM8 expression conferred poor survival in gliomas (Figure 1G). Analysis of transcript expression in Repository of Molecular Brain Neoplasia Data (REMBRANDT database) revealed TEM8 up-regulation in lower-grade gliomas (LGGs) and glioblastomas (Supplementary Figure 1E). This correlated with up-regulation in other datasets, such as Bredel Brain and Sun Brain (Supplementary Figure 1F). Immunoblotting for TEM8 on glioblastoma tumor tissue lysates revealed a predominant ~63 kDa band, suggesting that this is the transmembrane isoform expressed in glioblastomas (Figure 1H). Additionally, to determine TEM8 protein expression in non-neoplastic brain tissues, we utilized a control brain tissue microarray and observed no detectable staining in control brains (Supplementary Figure 1G), suggesting that TEM8 expression is negligible in normal brain, and its expression is correlated to gliomagenesis and its progression.

TEM8 expression regulates proliferation, invasion, migration, chemoresistance and radiation resistance in glioblastoma cells. To understand the functional consequences of TEM8 expression in glioblastomas, we overexpressed a 3X Flag-hTEM8/pcDNA3.1 construct in U87-MG, A172 and LN229 cell lines (Figure 2A). We observed a predominant band of 63 kDa, confirming expression of the transmembrane isoform, while also observing another band at 25 kDa (*), similar to our observations in glioblastoma tumor lysates (Figure 1H), suggesting that this could be a cleaved isoform produced in glioblastoma cells.

In Boyden-chamber assays, we observed increased invasion in TEM8 overexpressing cells (Figure 2B); while gelatin zymography using conditioned media revealed expression of active MMP-2 (Figure 2C) suggesting a possible role in increased invasion. We also observed increased wound-healing (Figure 2D), and increased neurosphere number and size in TEM8 overexpressing cells (Figure 2E). Using the MTT assay we explored if TEM8 expression enhanced chemo-resistance in cells towards four chemotherapeutic drugs viz. Temozolomide, Cisplatin, Etoposide, and 5-FluoroUracil (Figure 2F). Relative 50% Inhibitory Concentration (IC_{50}) calculations by non-linear regression curve fitting revealed increased IC_{50} values for all the

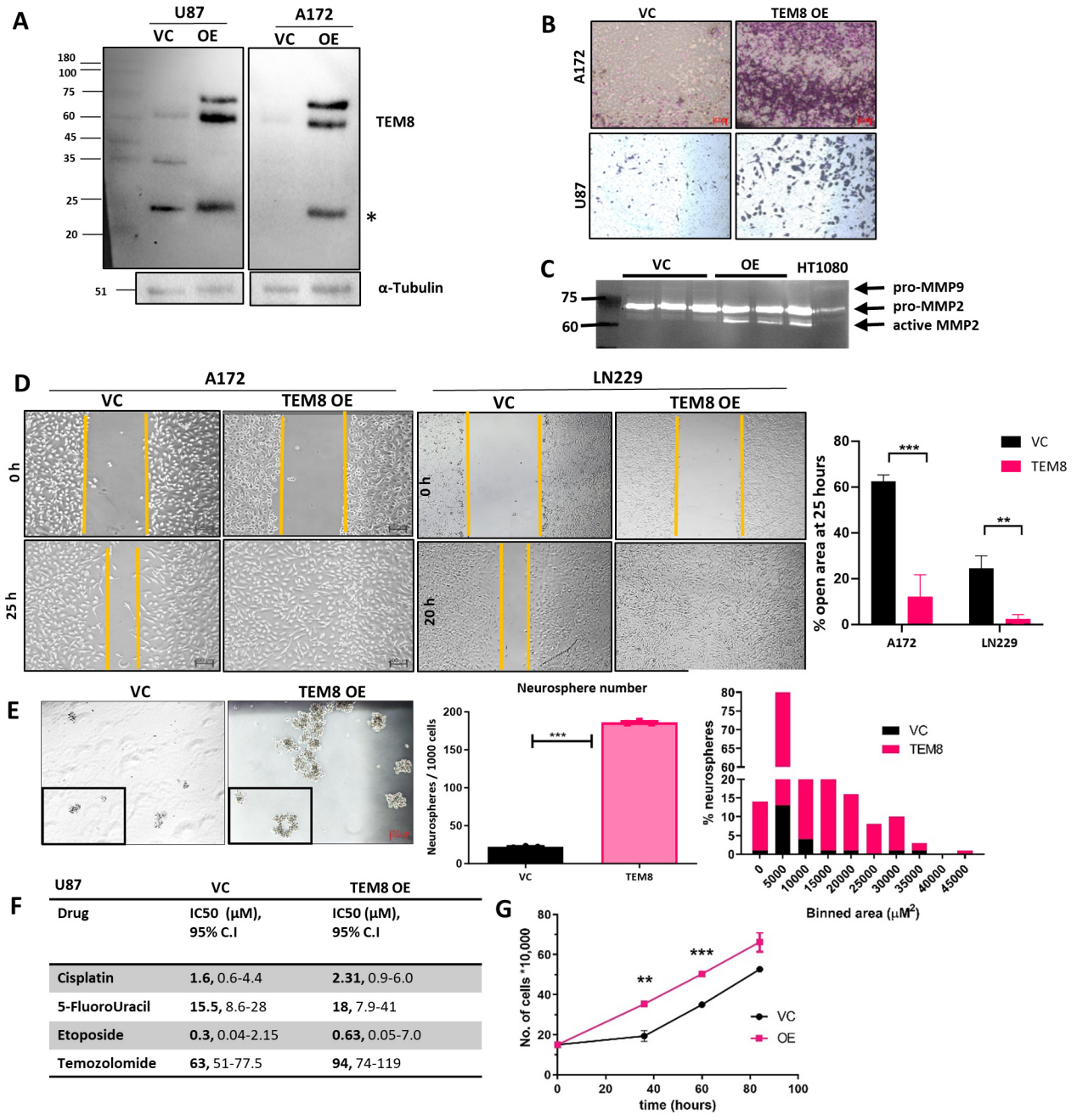

Figure 2. *Continued*

above drugs in TEM8 OE cells except in the case of 5-FluoroUracil, which showed a marginal increase (Supplementary Figure S2A).

We observed increased proliferation in TEM8 overexpressing (OE) cells compared to vector controls (VC) as seen by Trypan-blue based viability assays (Figure 2G) and BromodeoxyUridine uptake for 4 h (Supplementary Figure S2B), suggesting that TEM8 expression may regulate cell cycle progression. To assess that, we exposed stably overexpressing U87-MG glioma cells to prolonged (72 h) serum-starvation induced cell cycle synchronization (termed 0 h), and then stimulated cell cycle reentry with 10% FBS-containing complete media for 12 h (termed 12h) (Figure 2H). Quantitation from three independent experiments (Figure 2I) revealed that after 72 h of serum-starvation (time 0 h), ~92% of VC cells while 85% of TEM8 OE cells were G_1-phase arrested. A significantly higher percentage of cells in S phase were detected in TEM8 OE cells (~7%) compared to VC cells, suggesting a proportion of TEM8 OE

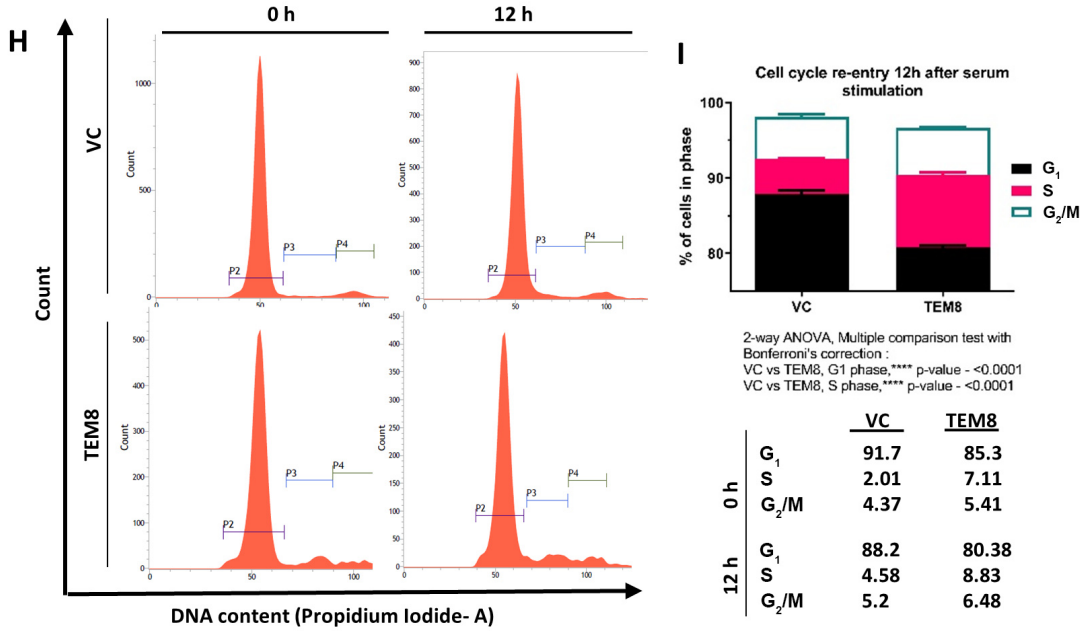

		VC	TEM8
0 h	G_1	91.7	85.3
	S	2.01	7.11
	G_2/M	4.37	5.41
12 h	G_1	88.2	80.38
	S	4.58	8.83
	G_2/M	5.2	6.48

Figure 2. *TEM8 gene induces increased proliferation, invasion, migration and chemoresistance. VC denotes vector control and OE denotes overexpression. (A) Representative TEM8 overexpression blots in U87 and A172, representing the transmembrane bound receptor. The extra band at 25 kDa (*) is presumably a cleavage product. (B) Representative Matrigel invasion assay in TEM8 overexpressing A172 and U87 cells. (C) Gelatin zymography with VC and TEM8 OE conditioned media. HT1080 conditioned media used as positive control. (D) Representative images and quantitation of wound-healing assays in A172 and LN229 cells, represented as percentage of open area. (E) Neurosphere generation capacity of VC and TEM8 OE cells at 7 days. Representative images (left) and quantitation of the same. (F) Relative 50% inhibitory concentrations (IC50) of VC and TEM8 OE cells towards Temozolomide, Cisplatin, 5-Fluorouracil, and Etoposide. C.I, Confidence interval. (G) Trypan-blue based cell proliferation assay in VC and TEM8 OE U87 cells. (H-I) Cell cycle progression assay after 12 h of serum-stimulation in VC and OE cells. Cells were G_1-phase synchronized (86%-92%) with 72 h of serum-starvation, and then stimulated using 10% serum-containing complete media. Percentage of cells in each phase after 12 h of stimulation was quantified via flow cytometry and is denoted as numbers. p-Values indicate 2-way Analysis of Variance (ANOVA) with Bonferroni's correction. All experiments were repeated thrice, and representative results are shown. p-Value for Student's t-test, ***p<0.0001; **p<0.001; *p<0.05.*

cells escaping arrest and progressing to the G_2/M phase. At 12 h of growth-stimulation (time 12 h), we observed 8.83% cells in S phase in TEM8 OE cells compared to 4.58% in VC cells, and a proportionately higher number of cells in the G_2/M phase. TEM8 expression thus endowed cells with a proliferation advantage.

Similarly, when TEM8 was stably knocked-down in U251-MG glioma cells with two shRNAs, pLKO.1-D6 and pLKO.1-D9 (Figure 3A), we observed a growth lag in TEM8 knock down cells (Figure 3B) compared to scrambled-shRNA transfected cells (SCR). As described earlier, we used a similar approach of 72 h serum-starvation induced synchronization and subsequent cell-cycle re-entry with 10% FBS-containing complete media (Figure 3C). After 72 h of serum-starvation (termed 0 h), we observed more cells (76%) being arrested in G_1 phase in D6 and D9 compared to 61% cells in SCR controls. To ascertain if parental U251 cells showed similarly low levels of G_1-synchronization as SCR cells, we performed the same experiment with U251-parental cells which revealed that ~66% cells were G_1 arrested (Supplementary Figure 3A). This suggested that TEM8 knockdown led to more efficient G_1-arrest in D6 and D9 cells on prolonged serum-starvation. Additionally, only about 11% of both D6 and D9 knockdown cells were found in G_2/M phase, while ~22% of SCR cells were found in the G_2/M phase. Further, at 12 h of growth-stimulation, we observed 26.3% cells in G_2/M phase in SCR, compared to 15 and 16% in D6 and D9 cells respectively, suggesting that TEM8 knockdown delays cell cycle progression. Quantification from three independent experiments is shown in Figure 3C.

We also demonstrated reduced invasion (Figure 3D) and migration (Figure 3E) in D6 and D9 cells when compared to SCR, and gelatin zymography with conditioned media from these cells revealed reduced MMP2 levels in knockdown cells compared to SCR controls (Figure 3F). To assess whether TEM8 knockdown led to reduced chemo- and radioresistance, we performed MTT and clonogenic assays respectively. In response to temozolomide and Cisplatin, we found relative IC_{50} concentrations were reduced in D6 and D9 cells compared to SCR (Figure 3G, Supplementary Figure 3B). Additionally, clonogenic assays after γ-radiation

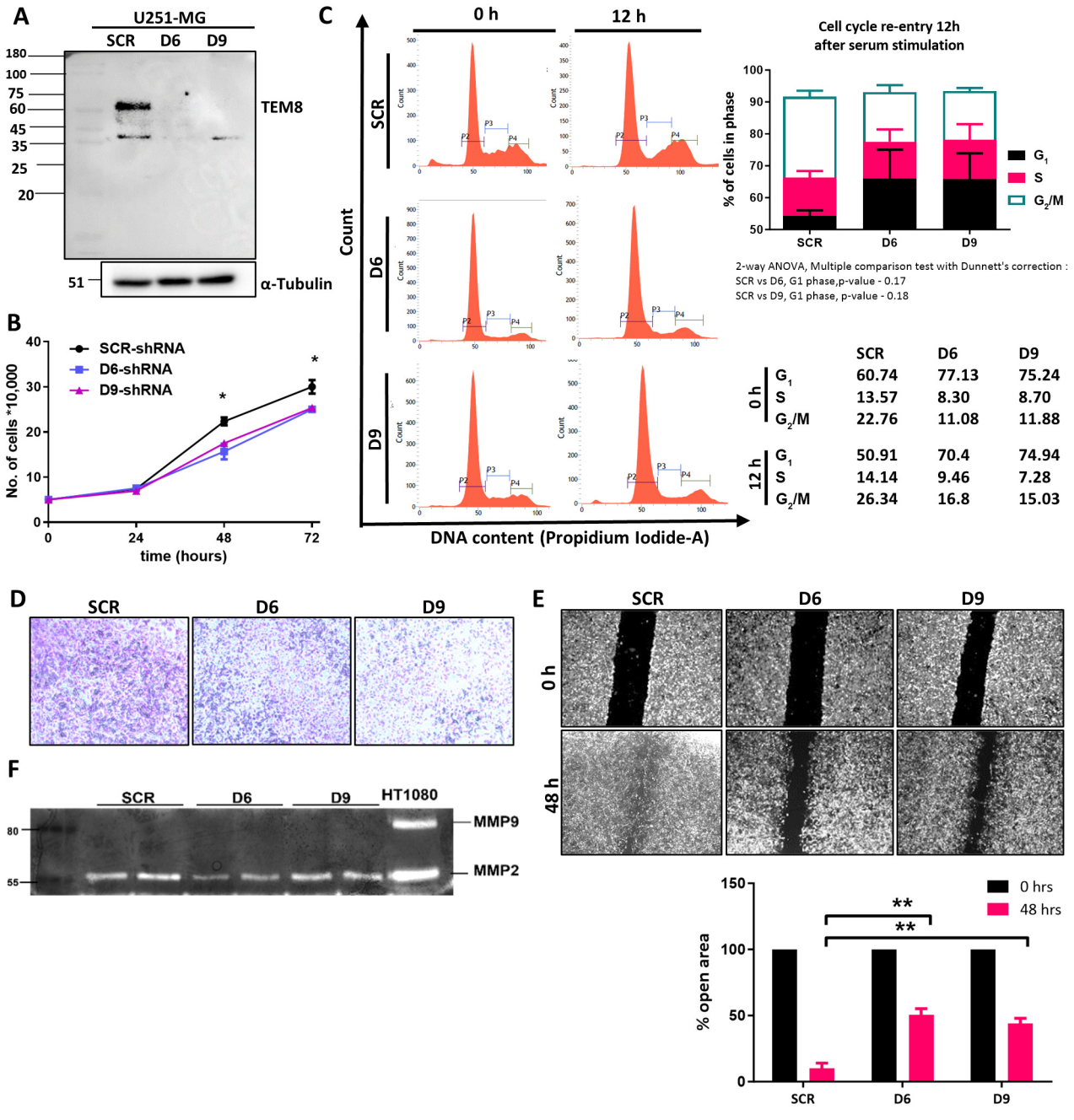

Figure 3. *Continued*

exposure (0-10 Gray) revealed that TEM8 knockdown D6 and D9 cells had attenuated radioresistance compared to SCR cells (Figure 3H), as evidenced by lesser area-under-curve (SCR:2.67, D6:1.98, D9:2.5) and surviving fraction.

The TEM8 gene regulates β-catenin signaling in glioblastoma cells. Few reports have suggested that *ANTXR1* can interact with LRP6 (33, 34), and engaging *ANTXR1* with the C5 fragment of Collagen VI or with Anthrax toxin component Protective Antigen, lead to induction of Wnt target genes, such as Axin2 or Zeb1 in triple-negative breast cancer or endothelial cells (28, 35). We, therefore, explored if TEM8 activation led to enhanced β-catenin signaling in glioblastoma cells. In U87 TEM8 OE cells, we observed induction of Wnt target genes Zeb1, Axin2, Nanog, Twist1 and α-SMA, although β-catenin or LRP6 transcript levels were unchanged

G

Drug	SCR IC50 (μM), 95 % C.I	D6 IC50 (μM), 95 % C.I	D9 IC50 (μM), 95 % C.I
Cisplatin	**12.2,** 7.6-19.3	**8.15,** 6.5-10	**7.2,** 4.9-10.4
Temozolomide	**251,** 177-403	**66.5,** 41-109	**204,** 152-297

H

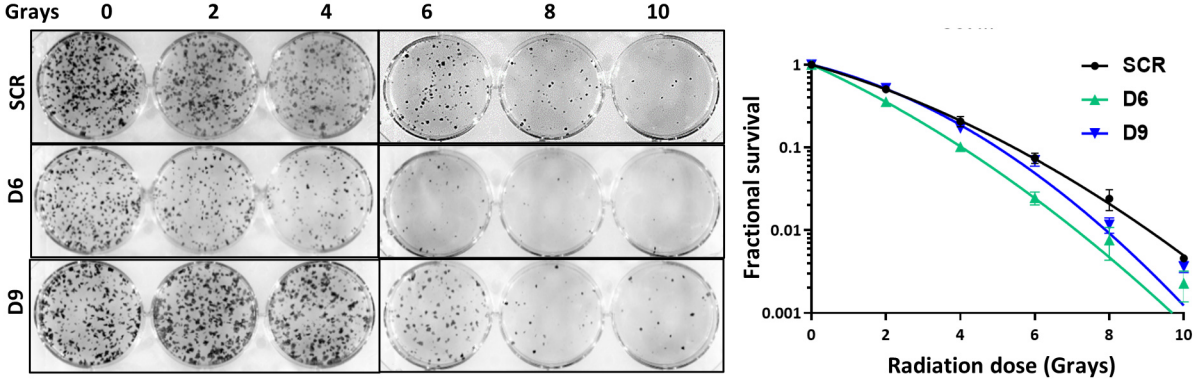

Figure 3. *TEM8 knockdown (D6 and D9) in U251-MG cells reduces proliferation, invasion, migration while increasing chemo- and radiosensitivity. SCR denotes scrambled controls while D6 and D9 are pooled knockdown cells. (A) Immunoblot showing TEM8 stable knockdown in U251 cells by lentiviral transduction. (B) Trypan-blue based cell proliferation assay in SCR and TEM8 knockdown cells. (C) Cell cycle progression assay after 12 h of serum-stimulation in SCR and knockdown cells. Cells were G_1-phase synchronized with 72 h of serum-starvation, and then stimulated using 10% serum-containing complete media. Percentage of cells in each phase after 12 h of stimulation was quantified via flow cytometry and is denoted as numbers. (D) Matrigel invasion assay in scrambled and TEM8 knockdown cells. (E) Wound-healing assay in U251 scrambled and TEM8 knockdown cells. Quantification represented as percentage of open area. (F) Gelatin zymography with conditioned media from scrambled and knockdown cells. HT1080 conditioned media used as positive control. (G) Relative 50% inhibitory concentrations (IC_{50}) of scrambled and knockdown cells for Temozolomide and Cisplatin. C.I, confidence interval. (H) Clonogenic assay in scrambled and TEM8 knockdown cells after exposure to 0-10 Grays of ionizing radiation. All experiments were repeated thrice, and representative results are shown. p-Value for Student's t-test, ***p<0.0001; **p<0.001; *p<0.05.*

(Figure 4A). In three glioma cell lines U87, LN229 and A172, we found induction of Zeb1, Twist, Vimentin, Oct4 and α-SMA, all of which are induced by β-catenin (Figure 4B). To determine if this association held true in patients, we assessed the co-expression of TEM8 with β-catenin target genes in glioblastoma patients from the Chinese Glioma Genome Atlas (CGGA) dataset in Gliovis. The expression of Zeb1, Axin1, Axin2, CyclinD1, c-myc and Vimentin were all positively correlated (Pearson's correlation co-efficient r^2: 0.33-0.77) to *ANTXR1/TEM8* expression (Figure 4C).

We observed no induction of canonical (Wnt1, Wnt2) or non-canonical (Wnt4, Wnt11) Wnt ligands (Figure 4D) in TEM8 OE cells, suggesting that β-catenin induction by TEM8 is likely Wnt-ligand independent. We further confirmed enhanced nuclear β-catenin accumulation in U87 and LN229 OE cells *via* nuclear-cytoplasmic fractionation (Figure 4E). Next, we utilized a dual-luciferase assay to measure nuclear β-catenin activity in overexpressing and knockdown cells. β-catenin responsive 7X TCF containing luciferase reporter construct, Super8X pTOPFlash, and its negative control with 7X mutated TCF, pFOPFlash, was transfected into these cells. We observed basally increased luciferase expression in TEM8 OE cells (Figure 4F) and reduced expression in D6 and D9 knockdown cells compared to SCR cells (Figure 4G), suggesting that TEM8 expression is correlated to nuclear β-catenin activity. Additionally, we found reduced protein levels of β-catenin target genes, such as Zeb1, Twist1, α-SMA, Vimentin in U251-D6 and -D9 knockdown cells (Figure 4F), suggesting transcriptional changes and enhanced activation of the β-catenin pathway in glioma cells.

TEM8 regulation of β-catenin occurs via Src/PI3K/AKT/GSK3β cascade in glioblastoma cells. As TEM8 could up-regulate β-catenin and its effector genes, and as per our data Wnt ligands may not be involved (Figure 4D), we explored the signaling pathway responsible for β-catenin translocation into the nucleus. We, therefore, determined the phosphorylation of protein kinases such as GSK3β, whose inactivating phosphorylation at Ser9 leads to β-catenin stabilization. Expectedly, p-GSK3β Ser 9 levels in TEM8 OE cells was up-

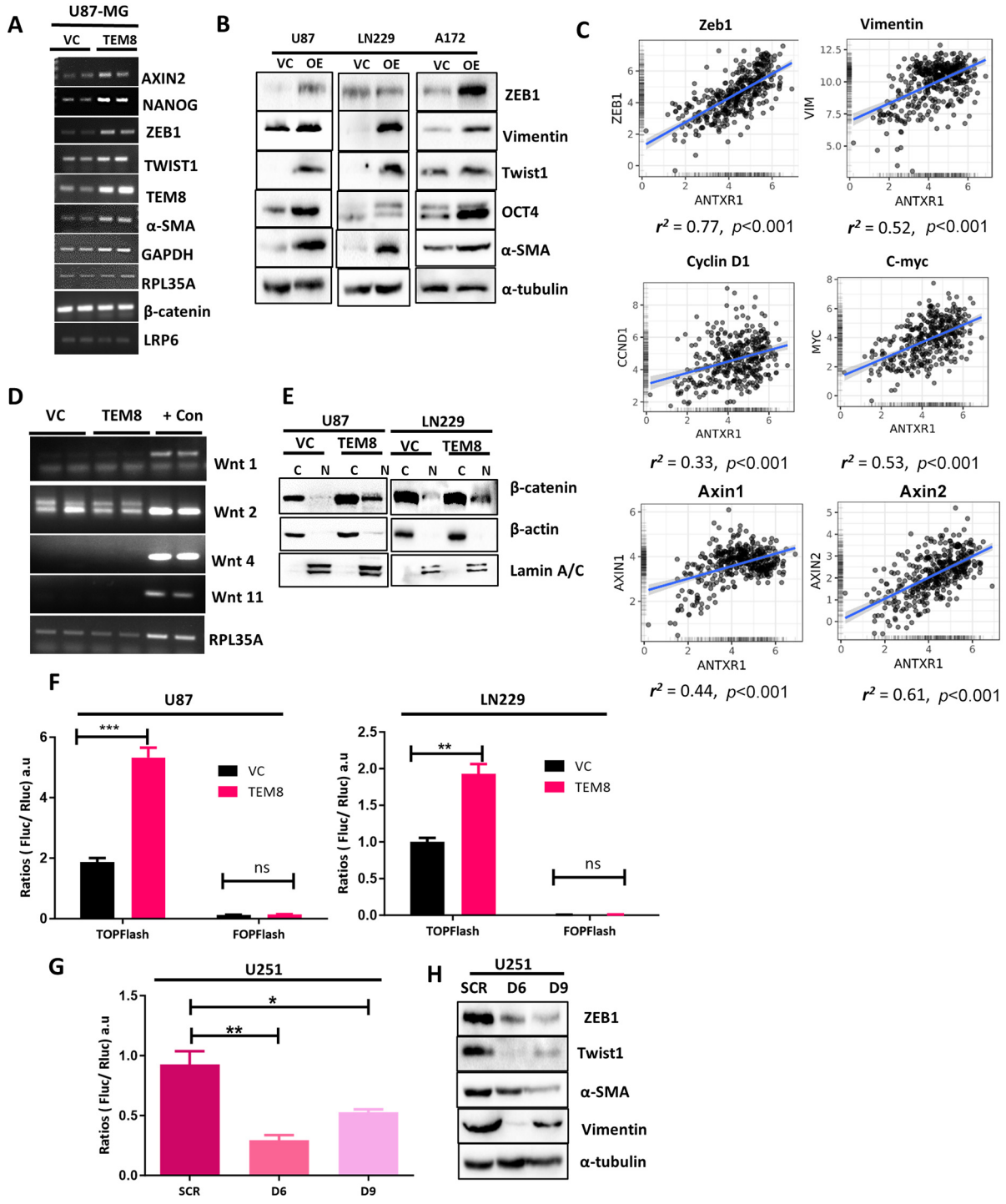

Figure 4. *TEM8 expression induces β-catenin in glioblastoma cells. (A) RNA expression of β-catenin target genes, such as Axin2, Twist, Nanog, Zeb1, α-SMA in VC and TEM8 OE cells via RT-PCR. (B) Immunoblotting for protein expression of β-catenin target genes, such as ZEB1, Twist, Vimentin, α-smooth muscle actin, OCT4 in VC and OE cells. (C) Gene co-expression analysis of ANTXR1/TEM8 with β-catenin target genes, such as Zeb1, Vimentin, Axin1, Axin2, CyclinD1, c-myc from the Chinese Glioma Genome Atlas (CGGA) dataset. (D) Expression of canonical (Wnt1, Wnt2) and non-canonical (Wnt4, Wnt11) Wnt ligand genes in TEM8 overexpressing cells. PCRs were conducted at saturating cycles, '+Con' denotes positive control (hFhTERT cDNA). (E) Nuclear-cytoplasmic fractionation assays in LN229 and U87 cells to determine β-catenin localization in VC and TEM8 OE cells. C, Cytoplasmic fraction; N, nuclear fraction. (F) Luciferase reporter assay with TOPFlash in VC and TEM8 OE cells, FOPFlash is used as negative control. ns, Non-significant. (G) Luciferase reporter assay with TOPFlash in scrambled controls and TEM8 knockdown cells. (H) Immunoblotting for protein expression of β-catenin targets, such as ZEB1, Twist, Vimentin expression in U251 scrambled and TEM8 knockdown cells.*

regulated (Figure 5A) in three cell lines: U87, LN229 and A172, concomitant with up-regulated β-catenin levels. GSK3β is regulated by varied upstream kinases, such as PI3 Kinase induced AKT (36, 37), Integrin-linked kinase (38, 39) or focal adhesion kinase (40) in glioblastomas. We observed elevated levels of phospho-AKT S473 and T308 in TEM8 OE cells. Additionally, we observed elevated phospho-ILK (S246) and phospho-FAK (Y397) levels in TEM8 OE cells.

In TEM8-knockdown cells, we observed a concomitant decrease in p-AKT (S473, T308), p-FAK (Y397) and p-GSK3β (S9) levels (Figure 5B). Interestingly, the total levels of FAK were reduced in knockdown cells, suggesting destabilization of focal adhesions and reduction of focal adhesion-mediated survival signals in these cells.

Since multiple kinases were induced, we utilized a panel of small-molecule inhibitors to identify the exact signaling cascade involved in β-catenin stabilization in the presence of TEM8: LY294002 (PI3K inhibitor), CPD-22 (ILK inhibitor), FAK inhibitor 1 (324877), RGD peptide (GRDGNP), PP2 (Src inhibitor) and PP3, a non-functional analog of PP2 was used as a negative control. We observed that phosphorylation on AKT (both T308 and S473) and GSK3β (S9) was abrogated in presence of PI3 kinase inhibitor LY294002 (Figure 5C), suggesting PI3 kinase activation was responsible for induction of p-AKT in TEM8 OE cells. Additionally, we observed that PP2 (Src kinase family inhibitor) abrogated p-AKT and p-GSK3β induction as well, suggesting that Src-dependent activation of PI3 Kinase/AKT was responsible for inactivating phosphorylation of GSK3β and stabilization of β-catenin in TEM8 OE cells. We therefore surmise that a non-canonical Src/PI3K/AKT/GSK3β/β-catenin pathway is activated in TEM8 expressing glioma cells (Figure 5D) which leads to enhanced proliferation, invasion, migration, chemo- and radioresistance in glioma cells.

Discussion

In this study, we investigated genome-wide methylation patterns in treatment-naïve and treated glioblastomas to assess promoter associated DNA methylation changes when glioblastomas recur. We report that *ANTXR1/TEM8* is a hypomethylated and up-regulated gene in recurrent GBMs, and we demonstrate increased protein expression in a retrospective cohort of paired primary-recurrent glioblastomas. *In vitro* studies in multiple glioma cell lines revealed that TEM8 expression conferred proliferation advantage, invasion, migration, chemoresistance and radioresistance in these cells. *TEM8*-knockout in multiple cell lines, such as melanoma, lung, colon has been demonstrated to lead to a drastic reduction in subcutaneous tumor growth (41). To our knowledge, this is the first study demonstrating TEM8's protumorigenic actions in glioblastoma. We demonstrate that the 63 kDa TEM8 isoform (sv1, membrane-bound receptor) is predominantly expressed in glioblastoma patient tissues and cell lines. It can potently regulate proliferation, invasion and migration in glioma cells, which is clinically relevant as one of the major causes of glioblastoma relapse and the tumor's ability to invade far away from the tumor bed. TEM8 expression was also found to influence chemo- and radioresistance of glioma cell lines. We also demonstrate the involvement of β-catenin in this protumorigenic phenotype and implicate a Src/PI3K/ AKT/GSK3β/β-catenin pathway in TEM8 expressing glioblastoma cells. Similar atypical regulation as this, *i.e.*, Src/PI3K/AKT/GSK3β/β-catenin was found in transmembrane-bound IL15 receptor signaling in renal cancer (42), suggesting that this might be a non-canonical pathway for β-catenin stabilization. The stimulus for signaling through Src/PI3K/AKT/GSK3β/β-catenin by TEM8 is not known from our study. We speculate that TEM8 is activated by endotrophin [cleaved C5 domain of Collagen α3(VI)]. This is because Col α3(VI) was demonstrated to bind the TEM8 extracellular domain (43) and is predominantly expressed in glioblastoma perivascular regions (44).

Interestingly, we found enhanced phosphorylation of Focal Adhesion Kinase (FAK) and Integrin-linked kinase (ILK) in TEM8-expressing glioma cells. It is reported that TEM8 mediates cellular adhesion (45), however the mechanism for this regulation is not clear. The finding from our study that FAK/ILK are activated by TEM8 may explain how TEM8 regulates cellular adhesion and positively impacts migration and invasion (31, 46).

We restricted this study to IDH-wildtype GBMs as IDH mutation confers a distinct CpG-hypermethylated phenotype (47), which may complicate data interpretation. In the recent past, Klughammer and Keisel *et al*. (48) and Kraboth *et al*. (49) reported exploring DNA methylation patterns in sequential glioblastomas. Both these studies utilized formalin-fixed paraffin embedded (FFPE) patient tissues, and a modified reduced representation bisulfite sequencing (RRBS) approach to probe DNA methylation at CpG-rich regions. The Klughammer study reported DNA methylation patterns related to immune cell infiltration and a loss of methylation at Wnt signaling related gene promoters. This has parallels with our study wherein we see differential methylation of immune system related genes like Interleukin receptor antagonists (*ILRN1)* and Interleukin ligands, and hypomethylation of the TEM8 gene leading to non-canonical stabilization of β-catenin levels in glioma cells.

One important aspect revealed from the study is that several different potassium-based voltage-gated ion-channels and solute-carrier channels were differentially methylated in recurrent compared to primary glioblastomas (Supplementary Figure 1, Supplementary Table I). Potassium channel dysregulation in cancer progression is frequently reported (50), and in glioblastomas in particular, they are known to modulate cellular osmolarity and consequently cellular volume; essential for tumor cell invasion in restricted spaces

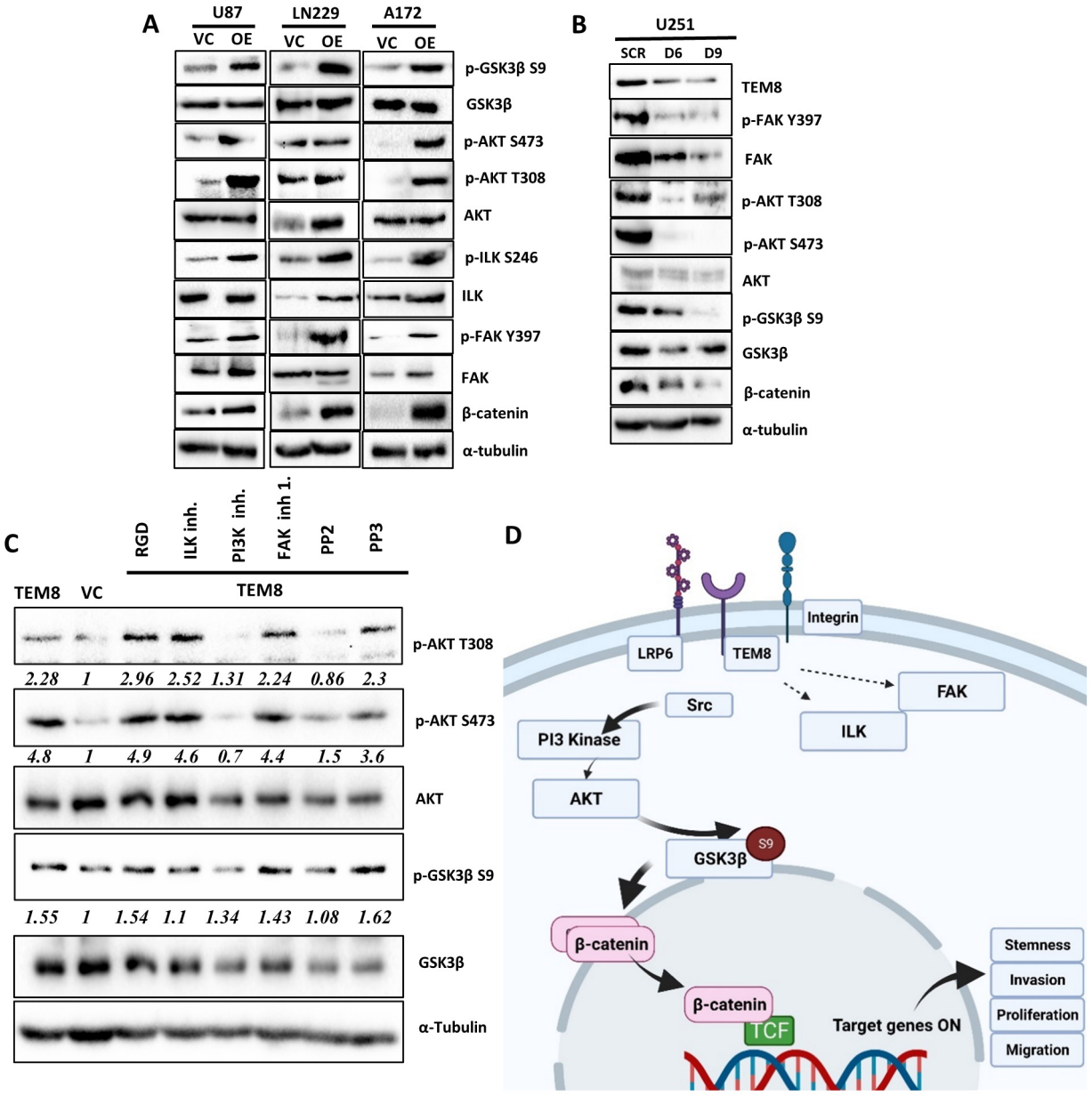

Figure 5. *Signaling cascade upon TEM8 activation. VC denotes vector control and OE denotes overexpression. (A) Immunoblotting for p-AKT, p-FAK, p-ILK, p-GSK3β, β-catenin, in VC and TEM8 OE cells. (B) Immunoblotting for p-AKT, p-GSK3β and β-catenin in scrambled controls and TEM8 knockdown cells. (C) Immunoblotting for assessing p-AKT T308, p-AKT S473 and p-GSK3β S9 levels in inhibitor treated cells for 6 h. (D) A model for Src/PI3K/AKT/GSK3β/β-catenin cascade in glioblastoma cells. Schematic created in BioRender.*

(51). Hence, the contribution of such genes in glioblastoma progression needs further investigation.

One of the limitations of this study is the cohort size of paired primary and recurrent patient samples, due to scarce availability of fresh-frozen paired samples. To mitigate this limitation, we utilized a separate cohort of retrospective paired FFPE tissues for independent validation of protein markers wherever necessary.

Conclusion

This study highlights the importance of epigenetic changes that promotes aggressive growth and invasion of glioma cells. We demonstrate the importance of one such gene, *TEM8* and there could be several other genes which may individually and/or collectively contribute to the recurrence phenomena. In this study, we have characterized the contribution of one such gene

in promoting glioblastoma aggressiveness and deciphered its mechanism (s) of action. Our study is in concordance with a growing body of literature suggesting that ionizing radiation and chemotherapy with alkylating agents as Temozolomide on highly heterogenous and adaptive tumors as glioblastomas may bring about complex and unpredictable responses, therefore newer and more efficient treatment modalities are urgently required for glioblastoma treatment.

Supplementary Material

Supplementary Figures (Figures S1-S3) and Tables (Supplementary Tables I-III) are available at: https://figshare.com/s/bed4395572648837fcae

Conflicts of Interest

The Authors declare that the research was conducted in the absence of any commercial or financial relationships that could be construed as a potential conflict of interest.

Authors' Contributions

P. Kundu contributed to the design, data acquisition, analysis, and interpretation, and drafted the manuscript; RJ contributed to bioinformatic analysis of methylation data; NKN contributed to sample collation; AA contributed to sample acquisition and clinical support; VS contributed to sample collation, immunohistopathology and clinical support. P. Kondaiah contributed to the design, data interpretation and manuscript writing. All Authors critically revised the manuscript. All Authors gave final approval and agreed to be accountable for all aspects of the work.

Acknowledgements

The authors acknowledge The Chinese Glioma Genome Atlas (CGGA), Gliovis, Oncomine and the REMBRANDT (Repository of Brain Neoplasia database) databases for data usage. The authors acknowledge Prof. G. Subba Rao, Indian Institute of Science for providing shRNAs, Mr. M.R Chandrasekhar for help with immunohistochemistry slides, Harsha Sugur for patient information, S Biswas for cluster diagram, and the central flow-cytometry facility, Biological Sciences, Indian Institute of Science. Paturu Kondaiah is a recipient of senior scientist fellowship from Indian National Science Congress.

Funding

The Department of Biotechnology, India (Grant No. BT/PR15885/MED/30/1754/2016), is acknowledged for funding.

References

1 Minniti G, Amelio D, Amichetti M, Salvati M, Muni R, Bozzao A, Lanzetta G, Scarpino S, Arcella A, Enrici RM: Patterns of failure and comparison of different target volume delineations in patients with glioblastoma treated with conformal radiotherapy plus concomitant and adjuvant temozolomide. Radiother Oncol 97(3): 377-381, 2010. DOI: 10.1016/j.radonc.2010.08.020

2 Tada T, Minakuchi K, Koda M, Kozuka T, Nishita T, Inoue Y, Hakuba A, Nakajima T, Onoyama Y: Patterns of recurrence after complete remission with definitive radiotherapy in the treatment of malignant glioma. Int J Clin Oncol 3(1): 36-40, 1998. DOI: 10.1007/BF02490100

3 Choucair AK, Levin VA, Gutin PH, Davis RL, Silver P, Edwards MSB, Wilson CB: Development of multiple lesions during radiation therapy and chemotherapy in patients with gliomas. J Neurosurg 65(5): 654-658, 1986. DOI: 10.3171/jns.1986.65.5.0654

4 Stupp R, Mason WP, van den Bent MJ, Weller M, Fisher B, Taphoorn MJ, Belanger K, Brandes AA, Marosi C, Bogdahn U, Curschmann J, Janzer RC, Ludwin SK, Gorlia T, Allgeier A, Lacombe D, Cairncross JG, Eisenhauer E, Mirimanoff RO, European Organisation for Research and Treatment of Cancer Brain Tumor and Radiotherapy Groups, National Cancer Institute of Canada Clinical Trials Group: Radiotherapy plus concomitant and adjuvant temozolomide for glioblastoma. N Engl J Med 352(10): 987-996, 2005. DOI: 10.1056/NEJMoa043330

5 Auffinger B, Tobias AL, Han Y, Lee G, Guo D, Dey M, Lesniak MS, Ahmed AU: Conversion of differentiated cancer cells into cancer stem-like cells in a glioblastoma model after primary chemotherapy. Cell Death Differ 21(7): 1119-1131, 2014. DOI: 10.1038/cdd.2014.31

6 Lee G, Auffinger B, Guo D, Hasan T, Deheeger M, Tobias AL, Kim JY, Atashi F, Zhang L, Lesniak MS, James CD, Ahmed AU: Dedifferentiation of glioma cells to glioma stem-like cells by therapeutic stress-induced HIF signaling in the recurrent GBM model. Mol Cancer Ther 15(12): 3064-3076, 2016. DOI: 10.1158/1535-7163.MCT-15-0675

7 Baisiwala S, Auffinger B, Caragher SP, Shireman JM, Ahsan R, Lee G, Hasan T, Park C, Saathoff MR, Christensen AC, Ahmed AU: Chemotherapeutic stress induces transdifferentiation of glioblastoma cells to endothelial cells and promotes vascular mimicry. Stem Cells Int 2019: 6107456, 2019. DOI: 10.1155/2019/6107456

8 Bao S, Wu Q, McLendon RE, Hao Y, Shi Q, Hjelmeland AB, Dewhirst MW, Bigner DD, Rich JN: Glioma stem cells promote radioresistance by preferential activation of the DNA damage response. Nature 444(7120): 756-760, 2006. DOI: 10.1038/nature05236

9 Dahan P, Martinez Gala J, Delmas C, Monferran S, Malric L, Zentkowski D, Lubrano V, Toulas C, Cohen-Jonathan Moyal E, Lemarie A: Ionizing radiations sustain glioblastoma cell dedifferentiation to a stem-like phenotype through survivin: possible involvement in radioresistance. Cell Death Dis 5(11): e1543, 2014. DOI: 10.1038/cddis.2014.509

10 Minata M, Audia A, Shi J, Lu S, Bernstock J, Pavlyukov MS, Das A, Kim SH, Shin YJ, Lee Y, Koo H, Snigdha K, Waghmare I, Guo X, Mohyeldin A, Gallego-Perez D, Wang J, Chen D, Cheng P, Mukheef F, Contreras M, Reyes JF, Vaillant B, Sulman EP, Cheng SY, Markert JM, Tannous BA, Lu X, Kango-Singh M, Lee LJ, Nam DH, Nakano I, Bhat KP: Phenotypic plasticity of invasive edge glioma stem-like cells in response to ionizing radiation. Cell Rep 26(7): 1893-1905.e7, 2019. DOI: 10.1016/j.celrep.2019.01.076

11 Osuka S, Van Meir EG: Overcoming therapeutic resistance in glioblastoma: the way forward. J Clin Invest 127(2): 415-426, 2017. DOI: 10.1172/JCI89587

12 Yoon N, Kim HS, Lee JW, Lee EJ, Maeng LS, Yoon WS: Targeted genomic sequencing reveals different evolutionary

patterns between locally and distally recurrent glioblastomas. Cancer Genomics Proteomics 17(6): 803-812, 2020. DOI: 10.21873/cgp.20234

13 Johnson BE, Mazor T, Hong C, Barnes M, Aihara K, McLean CY, Fouse SD, Yamamoto S, Ueda H, Tatsuno K, Asthana S, Jalbert LE, Nelson SJ, Bollen AW, Gustafson WC, Charron E, Weiss WA, Smirnov IV, Song JS, Olshen AB, Cha S, Zhao Y, Moore RA, Mungall AJ, Jones SJM, Hirst M, Marra MA, Saito N, Aburatani H, Mukasa A, Berger MS, Chang SM, Taylor BS, Costello JF: Mutational analysis reveals the origin and therapy-driven evolution of recurrent glioma. Science 343(6167): 189-193, 2014. DOI: 10.1126/science.1239947

14 Antwih DA, Gabbara KM, Lancaster WD, Ruden DM, Zielske SP: Radiation-induced epigenetic DNA methylation modification of radiation-response pathways. Epigenetics 8(8): 839-848, 2013. DOI: 10.4161/epi.25498

15 Barciszewska AM, Gurda D, Głodowicz P, Nowak S, Naskręt-Barciszewska MZ: A new epigenetic mechanism of temozolomide action in glioma cells. PLoS One 10(8): e0136669, 2015. DOI: 10.1371/journal.pone.0136669

16 Thienpont B, Steinbacher J, Zhao H, D'Anna F, Kuchnio A, Ploumakis A, Ghesquière B, Van Dyck L, Boeckx B, Schoonjans L, Hermans E, Amant F, Kristensen VN, Peng Koh K, Mazzone M, Coleman M, Carell T, Carmeliet P, Lambrechts D: Tumour hypoxia causes DNA hypermethylation by reducing TET activity. Nature 537(7618): 63-68, 2016. DOI: 10.1038/nature19081

17 Shahrzad S, Bertrand K, Minhas K, Coomber BL: Induction of DNA hypomethylation by tumor hypoxia. Epigenetics 2(2): 119-125, 2007. DOI: 10.4161/epi.2.2.4613

18 Morris TJ, Butcher LM, Feber A, Teschendorff AE, Chakravarthy AR, Wojdacz TK, Beck S: ChAMP: 450k chip analysis methylation pipeline. Bioinformatics 30(3): 428-430, 2014. DOI: 10.1093/bioinformatics/btt684

19 Somasundaram K, Reddy SP, Vinnakota K, Britto R, Subbarayan M, Nambiar S, Hebbar A, Samuel C, Shetty M, Sreepathi HK, Santosh V, Hegde AS, Hegde S, Kondaiah P, Rao MRS: Upregulation of ASCL1 and inhibition of Notch signaling pathway characterize progressive astrocytoma. Oncogene 24(47): 7073-7083, 2005. DOI: 10.1038/sj.onc.1208865

20 Yang MY, Chaudhary A, Seaman S, Dunty J, Stevens J, Elzarrad MK, Frankel AE, St Croix B: The cell surface structure of tumor endothelial marker 8 (TEM8) is regulated by the actin cytoskeleton. Biochim Biophys Acta 1813(1): 39-49, 2011. DOI: 10.1016/j.bbamcr.2010.11.013

21 Gebäck T, Schulz MMP, Koumoutsakos P, Detmar M: TScratch: a novel and simple software tool for automated analysis of monolayer wound healing assays. Biotechniques 46(4): 265-274, 2009. DOI: 10.2144/000113083

22 Chapnick DA, Liu X: Analysis of ligand-dependent nuclear accumulation of Smads in TGF-beta signaling. Methods Mol Biol 647: 95-111, 2010. DOI: 10.1007/978-1-60761-738-9_5

23 Schindelin J, Arganda-Carreras I, Frise E, Kaynig V, Longair M, Pietzsch T, Preibisch S, Rueden C, Saalfeld S, Schmid B, Tinevez JY, White DJ, Hartenstein V, Eliceiri K, Tomancak P, Cardona A: Fiji: an open-source platform for biological-image analysis. Nat Methods 9(7): 676-682, 2012. DOI: 10.1038/nmeth.2019

24 Low JY, Nicholson HD: Epigenetic modifications of caveolae associated proteins in health and disease. BMC Genet 16: 71, 2015. DOI: 10.1186/s12863-015-0231-y

25 Zhang W, Sun HC, Wang WQ, Zhang QB, Zhuang PY, Xiong YQ, Zhu XD, Xu HX, Kong LQ, Wu WZ, Wang L, Song TQ, Li Q, Tang ZY: Sorafenib down-regulates expression of HTATIP2 to promote invasiveness and metastasis of orthotopic hepatocellular carcinoma tumors in mice. Gastroenterology 143(6): 1641-1649.e5, 2012. DOI: 10.1053/j.gastro.2012.08.032

26 Cui T, Chen Y, Yang L, Knösel T, Zöller K, Huber O, Petersen I: DSC3 expression is regulated by p53, and methylation of DSC3 DNA is a prognostic marker in human colorectal cancer. Br J Cancer 104(6): 1013-1019, 2011. DOI: 10.1038/bjc.2011.28

27 Litan A, Langhans SA: Cancer as a channelopathy: ion channels and pumps in tumor development and progression. Front Cell Neurosci 9: 86, 2015. DOI: 10.3389/fncel.2015.00086

28 Chen D, Bhat-Nakshatri P, Goswami C, Badve S, Nakshatri H: ANTXR1, a stem cell-enriched functional biomarker, connects collagen signaling to cancer stem-like cells and metastasis in breast cancer. Cancer Res 73(18): 5821-5833, 2013. DOI: 10.1158/0008-5472.CAN-13-1080

29 Cao C, Wang Z, Huang L, Bai L, Wang Y, Liang Y, Dou C, Wang L: Down-regulation of tumor endothelial marker 8 suppresses cell proliferation mediated by ERK1/2 activity. Sci Rep 6: 23419, 2016. DOI: 10.1038/srep23419

30 Høye AM, Tolstrup SD, Horton ER, Nicolau M, Frost H, Woo JH, Mauldin JP, Frankel AE, Cox TR, Erler JT: Tumor endothelial marker 8 promotes cancer progression and metastasis. Oncotarget 9(53): 30173-30188, 2018. DOI: 10.18632/oncotarget.25734

31 Cai C, Dang W, Liu S, Huang L, Li Y, Li G, Yan S, Jiang C, Song X, Hu Y, Gu J: Anthrax toxin receptor 1/tumor endothelial marker 8 promotes gastric cancer progression through activation of the PI3K/AKT/mTOR signaling pathway. Cancer Sci 111(4): 1132-1145, 2020. DOI: 10.1111/cas.14326

32 Bowman RL, Wang Q, Carro A, Verhaak RG, Squatrito M: GlioVis data portal for visualization and analysis of brain tumor expression datasets. Neuro Oncol 19(1): 139-141, 2017. DOI: 10.1093/neuonc/now247

33 Abrami L, Kunz B, Deuquet J, Bafico A, Davidson G, van der Goot FG: Functional interactions between anthrax toxin receptors and the WNT signalling protein LRP6. Cell Microbiol 10(12): 2509-2519, 2008. DOI: 10.1111/j.1462-5822.2008.01226.x

34 Wei W, Lu Q, Chaudry GJ, Leppla SH, Cohen SN: The LDL receptor-related protein LRP6 mediates internalization and lethality of anthrax toxin. Cell 124(6): 1141-1154, 2006. DOI: 10.1016/j.cell.2005.12.045

35 Verma K, Gu J, Werner E: Tumor endothelial marker 8 amplifies canonical Wnt signaling in blood vessels. PLoS One 6(8): e22334, 2011. DOI: 10.1371/journal.pone.0022334

36 Cross DAE, Alessi DR, Cohen P, Andjelkovich M, Hemmings BA: Inhibition of glycogen synthase kinase-3 by insulin mediated by protein kinase B. Nature 378(6559): 785-789, 1995. DOI: 10.1038/378785a0

37 Atkins RJ, Dimou J, Paradiso L, Morokoff AP, Kaye AH, Drummond KJ, Hovens CM: Regulation of glycogen synthase kinase-3 beta (GSK-3β) by the Akt pathway in gliomas. J Clin Neurosci 19(11): 1558-1563, 2012. DOI: 10.1016/j.jocn.2012.07.002

38 Persad S, Attwell S, Gray V, Delcommenne M, Troussard A, Sanghera J, Dedhar S: Inhibition of integrin-linked kinase (ILK) suppresses activation of protein kinase B/Akt and induces cell cycle arrest and apoptosis of PTEN-mutant prostate cancer cells. Proc Natl Acad Sci USA 97(7): 3207-3212, 2000. DOI: 10.1073/pnas.97.7.3207

39 Edwards LA, Thiessen B, Dragowska WH, Daynard T, Bally MB, Dedhar S: Inhibition of ILK in PTEN-mutant human glioblastomas inhibits PKB/Akt activation, induces apoptosis, and delays tumor growth. Oncogene 24(22): 3596-3605, 2005. DOI: 10.1038/sj.onc.1208427

40 Patil SS, Gokulnath P, Bashir M, Shwetha SD, Jaiswal J, Shastry AH, Arimappamagan A, Santosh V, Kondaiah P: Insulin-like growth factor binding protein-2 regulates β-catenin signaling pathway in glioma cells and contributes to poor patient prognosis. Neuro Oncol 18(11): 1487-1497, 2016. DOI: 10.1093/neuonc/now053

41 Chaudhary A, Hilton MB, Seaman S, Haines DC, Stevenson S, Lemotte PK, Tschantz WR, Zhang XM, Saha S, Fleming T, St Croix B: TEM8/ANTXR1 blockade inhibits pathological angiogenesis and potentiates tumoricidal responses against multiple cancer types. Cancer Cell 21(2): 212-226, 2012. DOI: 10.1016/j.ccr.2012.01.004

42 Yuan H, Meng X, Guo W, Cai P, Li W, Li Q, Wang W, Sun Y, Xu Q, Gu Y: Transmembrane-bound IL-15-promoted epithelial-mesenchymal transition in renal cancer cells requires the Src-dependent Akt/GSK-3β/β-catenin pathway. Neoplasia 17(5): 410-420, 2015. DOI: 10.1016/j.neo.2015.04.002

43 Nanda A, Carson-Walter EB, Seaman S, Barber TD, Stampfl J, Singh S, Vogelstein B, Kinzler KW, St. Croix B: TEM8 interacts with the cleaved C5 domain of collagen α3(VI). Cancer Res 64(3): 817-820, 2004. DOI: 10.1158/0008-5472.CAN-03-2408

44 Turtoi A, Blomme A, Bianchi E, Maris P, Vannozzi R, Naccarato AG, Delvenne P, De Pauw E, Bevilacqua G, Castronovo V: Accessibilome of human glioblastoma: Collagen-VI-alpha-1 is a new target and a marker of poor outcome. J Proteome Res 13(12): 5660-5669, 2014. DOI: 10.1021/pr500657w

45 Werner E, Kowalczyk AP, Faundez V: Anthrax toxin receptor 1/tumor endothelium marker 8 mediates cell spreading by coupling extracellular ligands to the actin cytoskeleton. J Biol Chem 281(32): 23227-23236, 2006. DOI: 10.1074/jbc.M603676200

46 Hotchkiss KA, Basile CM, Spring SC, Bonuccelli G, Lisanti MP, Terman BI: TEM8 expression stimulates endothelial cell adhesion and migration by regulating cell?matrix interactions on collagen. Exp Cell Res 305(1): 133-144, 2005. DOI: 10.1016/j.yexcr.2004.12.025

47 Noushmehr H, Weisenberger DJ, Diefes K, Phillips HS, Pujara K, Berman BP, Pan F, Pelloski CE, Sulman EP, Bhat KP, Verhaak RG, Hoadley KA, Hayes DN, Perou CM, Schmidt HK, Ding L, Wilson RK, Van Den Berg D, Shen H, Bengtsson H, Neuvial P, Cope LM, Buckley J, Herman JG, Baylin SB, Laird PW, Aldape K, Cancer Genome Atlas Research Network: Identification of a CpG island methylator phenotype that defines a distinct subgroup of glioma. Cancer Cell 17(5): 510-522, 2010. DOI: 10.1016/j.ccr.2010.03.017

48 Klughammer J, Kiesel B, Roetzer T, Fortelny N, Nemc A, Nenning KH, Furtner J, Sheffield NC, Datlinger P, Peter N, Nowosielski M, Augustin M, Mischkulnig M, Ströbel T, Alpar D, Ergüner B, Senekowitsch M, Moser P, Freyschlag CF, Kerschbaumer J, Thomé C, Grams AE, Stockhammer G, Kitzwoegerer M, Oberndorfer S, Marhold F, Weis S, Trenkler J, Buchroithner J, Pichler J, Haybaeck J, Krassnig S, Mahdy Ali K, von Campe G, Payer F, Sherif C, Preiser J, Hauser T, Winkler PA, Kleindienst W, Würtz F, Brandner-Kokalj T, Stultschnig M, Schweiger S, Dieckmann K, Preusser M, Langs G, Baumann B, Knosp E, Widhalm G, Marosi C, Hainfellner JA, Woehrer A, Bock C: The DNA methylation landscape of glioblastoma disease progression shows extensive heterogeneity in time and space. Nat Med 24(10): 1611-1624, 2018. DOI: 10.1038/s41591-018-0156-x

49 Kraboth Z, Galik B, Tompa M, Kajtar B, Urban P, Gyenesei A, Miseta A, Kalman B: DNA CpG methylation in sequential glioblastoma specimens. J Cancer Res Clin Oncol 146(11): 2885-2896, 2020. DOI: 10.1007/s00432-020-03349-w

50 Comes N, Serrano-Albarrás A, Capera J, Serrano-Novillo C, Condom E, Ramón Y Cajal S, Ferreres JC, Felipe A: Involvement of potassium channels in the progression of cancer to a more malignant phenotype. Biochim Biophys Acta - Biomembr 1848(10): 2477-2492, 2015. DOI: 10.1016/j.bbamem.2014.12.008

51 Turner KL, Sontheimer H: Cl- and K+ channels and their role in primary brain tumour biology. Philos Trans R Soc Lond B Biol Sci 369(1638): 20130095, 2014. DOI: 10.1098/rstb.2013.0095

Received April 1, 2024
Revised May 20, 2024
Accepted June 10, 2024